Quantum Bayes classifiers and their application in image classification

Ming-Ming Wang[1,*] and Xiao-Ying Zhang[1]

[1] *The Shaanxi Key Laboratory of Clothing Intelligence, School of Computer Science, Xi'an Polytechnic University, Xi'an 710048, China*

(Dated: today)

Bayesian networks are powerful tools for probabilistic analysis and have been widely used in machine learning and data science. Unlike the time-consuming parameter training process of neural networks, Bayes classifiers constructed on Bayesian networks can make decisions based solely on statistical data from samples. In this paper, we focus on constructing quantum Bayes classifiers (QBCs). We design both a naïve QBC and three semi-naïve QBCs (SN-QBCs). These QBCs are then applied to image classification tasks. To reduce computational complexity, we employ a local feature sampling method to extract a limited number of feature attributes from an image. These attributes serve as nodes of the Bayesian networks to generate the QBCs. We simulate these QBCs on the MindQuantum platform and evaluate their performance on the MNIST and Fashion-MNIST datasets. Our results demonstrate that these QBCs achieve good classification accuracies even with a limited number of attributes. The classification accuracies of QBCs on the MNIST dataset surpass those of classical Bayesian networks and quantum neural networks that utilize all available feature attributes.

I. INTRODUCTION

As a powerful tool for studying causal relationships between variables and inferring the impact of variable states on outcomes, Bayesian networks are widely used in machine learning and data science, including Monte Carlo analysis [1], reliability and risk analysis [2], health monitoring [3], healthcare [4], and biomedical systems [5], etc. The size of a Bayesian network depends on the number of nodes and their dependencies [6]. Learning and inference in complex networks can be challenging, especially when dealing with large-scale Bayesian networks, which have been proven to be an NP-hard problem [7]. The emergence of quantum computing offers a new solution to this challenge.

In recent years, many quantum algorithms have demonstrated quantum supremacy for achieving certain accelerations over their classical counterparts. For example, the Shor's algorithm [8] achieves exponential acceleration in solving the large number factorization problem. The Grover's algorithm [9] achieves quadratic acceleration in searching the unstructured data. In addition, quantum algorithms based on classical machine learning, such as quantum support vector machine [10] and quantum K-nearest neighbor [11], have also demonstrated quantum accelerations. Image classification is a fundamental problem in computer vision. With the advancement of quantum machine learning, several quantum classifiers have been developed for image classification, including quantum convolutional neural networks [12–15], quantum K-nearest neighbor algorithm [11], and quantum ensemble methods [16–20], etc. Recent progresses of quantum classifiers could be found in [21].

Quantum Bayesian networks (QBN) were introduced in 1995 as a simulation of classical ones [22]. In 2013, Ozols et al. proposed a quantum version of the rejection sampling algorithm called quantum rejection sampling for Bayesian inference [23]. In 2016, Moreira and Wichert proposed a quantum-like Bayesian network that uses amplitudes to represent marginal and conditional probabilities [24]. In 2019, Woerner and Egger developed a quantum algorithm [25] for risk analysis using the principles of amplitude amplification and estimation. Their algorithm can provide a quadratic speed-up compared to classical Monte Carlo methods. In 2023, Gabriel et al. proposed a quantum algorithm based on quantum walks for quantum Bayesian estimation of gravitational waves parameters from black holes [26]. Recently, Borujeni et al. proposed a quantum circuit representation of Bayesian networks [27]. They designed quantum Bayesian networks for specific problems, such as stock prediction and liquidity risk assessment. Walid et al. further proposed an optimized version of quantum circuit for improving the quantum representation of Bayesian networks [28].

Currently, there is a lack of research on quantum Bayes classifiers (QBCs) building on Bayesian networks for solving image classification problems. Different from the parameters learning mode of neural networks, a Bayes classifier makes a classification decisions based only on sample features, without the tedious training process, resulting in lower computational complexity, faster speed, and less resource consumption. In this paper, we study the construction of

* bluess1982@126.com

quantum Bayes classifiers (QBCs). Specifically, we design a naïve [29, 30] QBC and three semi-naïve QBCs (SN-QBCs), i.e., the SN-QBC based on SPODE network [31, 32] with the attribute in the center of an image as the superfather, the SN-QBC based on TAN network [31, 32], and the SN-QBC based on symmetric relationship of attributes in an image. These QBCs are then applied to image classification tasks. We simulate these QBCs on the MindQuantum platform [33] and evaluate their performance on the MNIST [34] and Fashion-MNIST [35] datasets.

This paper is organized as follows. Sect. 2 introduces the basic concepts of Bayes classifiers. Sect. 3 discusses the constructions of QBCs. Sect. 4 presents the image classification algorithm based on QBCs. Sect. 5 demonstrates the simulation results of QBCs for image classification on the MNIST and Fashion-MNIST datasets. Sect. 6 further discusses and concludes the paper.

II. BAYES CLASSIFIER

A Bayes classifier is a statistical classifier based on Bayes' theorem. It considers selecting the optimal category label based on probabilities and misclassification losses, assuming that all relevant probabilities are known. Suppose the feature of a sample data is $X = \{x_1, x_2, \cdots, x_i, \cdots, x_n\}$ with x_i is an *attribute* of X, and the set of class labels is $Y = \{y_1, y_2, \cdots, y_i, \cdots, y_N\}$. Based on the *posterior probability* $P(y_i|X)$, the expected loss of classifying the sample with feature X as y_i is defined as [32]

$$R(y_i|X) = \sum_{j=1}^{N} \lambda_{ij} P(y_j|X), \tag{1}$$

where λ_{ij} is the misclassification loss. The Bayes classifier attempts to correctly classify new samples with minimal misclassification loss based on the distribution pattern of existing samples. The optimal Bayes classifier can be denoted as

$$D(X) = \arg\min_{y \in Y} R(y|X). \tag{2}$$

For a specific problem to minimize the misclassification rate, λ_{ij} can be written as

$$\lambda_{ij} = \begin{cases} 0, & \text{if } i = j; \\ 1, & \text{otherwise.} \end{cases} \tag{3}$$

Therefore, the optimal Bayes classifier can be rewritten as

$$D(X) = \arg\max_{y \in Y} P(y|X). \tag{4}$$

That is, the optimal Bayes classifier selects the class that maximizes the posterior probability $P(y|X)$ given the sample with feature X.

Obtaining an accurate posterior probability $P(y|X)$ is critical for a Bayes classifier, but this is often challenging in reality. In the probability framework, the posterior probability $P(y|X)$ can be estimated based on a finite number of training sample. According to Bayes' theorem [32], the posterior probability $P(y|X)$ can be written as

$$P(y|X) = \frac{P(X|y)P(y)}{P(X)} \tag{5}$$

where $P(X)$ is the evidence factor used for normalization, $P(y)$ is the *class-prior probability*, and $P(X|y)$ is the *class-conditional probability* of the sample X with respect to y. According to the law of large numbers [36], when there are a sufficient number of independently and identically distributed samples, $P(y)$ can be estimated by the frequency of each class that appears in the training set. As for the class-conditional probability $P(X|y)$, it involves combinations of all attributes in X. Assuming each attribute x_i has d possible values, $P(X|y)$ will have $N * d^n$ possible values.

A. Naïve Bayes Classifier

Clearly, it is difficult to obtain the *class-conditional probabilities* directly from a limited number of training sample, as it will result in the problem of combinatorial explosion in calculation, which becomes more severe with the increase

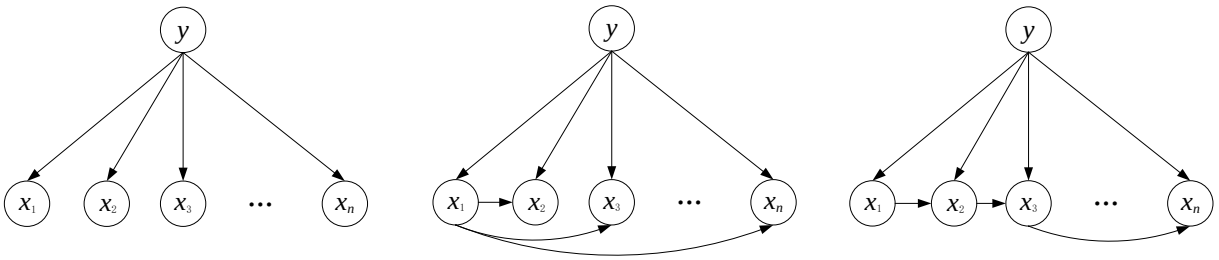

(a) Naïve. (b) SPODE. (c) TAN.

FIG. 1: Bayesian networks with different attributes dependencies.

of attributes. The naïve Bayes classifier [29, 30] is based on the assumption of "independence", which assumes that each attribute independently affects the classification result, as shown in Fig. (1a). In this case, Eq. (5) can be rewritten as

$$P(y|X) = \frac{P(y)\prod_i^n P(x_i|y)}{P(X)}, \tag{6}$$

where x_i the i-th attribute of X. Since all $P(X)$ are the same, the naïve Bayes classifier can be represented as

$$D_{\text{nb}} = \arg\max_{y\in Y} P(y)\prod_i^n P(x_i|y). \tag{7}$$

B. Semi-naïve Bayes Classifier

The premise of the naïve Bayes classifier is that all attributes satisfy the assumption of independence, but this is often not the case in practical applications. Therefore, the learning method of the semi-naïve Bayes classifier [31, 32] has emerged, which considers stronger dependencies between attributes while avoids the problem of combinatorial explosion caused by considering the joint probability distribution of all attributes. *One-Dependent Estimator* (ODE) is the most common strategy for the semi-naïve Bayes classifier, which assumes that each attribute only depends on at most one other attribute besides the label y, i.e.,

$$P(y|X) \propto P(y)\prod_i^n P(x_i|y, pa_i). \tag{8}$$

where pa_i is the dependent attribute (or parent attribute) of x_i. The key problem of the semi-naïve Bayes classifier is how to determine the parent attribute of x_i.

A typical approach is to assume that all attributes depend on a single attribute, referred to as the Super-Parent ODE (SPODE), whose dependency relationship is illustrated in Fig. (1b). An alternative method is the Tree Augmented Naïve Bayes (TAN), which calculates the conditional mutual information between any pair of attributes and constructs a maximum weighted tree [32, 37] based on the attribute dependencies, as depicted in Fig. (1c).

III. QUANTUM BAYES CLASSIFIERS

Unlike classical bits that can only represent either 0 or 1, a quantum bit (qubit) can represent both 0 and 1 simultaneously, i.e., quantum superposition. A single-qubit state can be represented as $|\varphi\rangle = \alpha|0\rangle + \beta|1\rangle$, where $|0\rangle$ and $|1\rangle$ are the basis states of the single-qubit, α and β are the amplitudes that satisfy the normalization condition $|\alpha|^2 + |\beta|^2 = 1$. When $|\varphi\rangle$ is measured in the computational basis $\{|0\rangle, |1\rangle\}$, the state will collapse into basis states $|0\rangle$ or $|1\rangle$ with the probability $|\alpha|^2$ or $|\beta|^2$, respectively. In the quantum gate computing model [38], quantum gates are used to represent unitary operations acting on qubits. Quantum gates can be divided into single-qubit gates and multi-qubit gates, and any multi-qubit gate can be decomposed into a set of universal quantum gates [38].

In this paper, a quantum circuit for a QBC is constructed using single-qubit gates R_y and X, and multi-qubit controlled gates C^nR_y. The X-gate is a flip gate that flips $|0\rangle$ to $|1\rangle$ or $|1\rangle$ to $|0\rangle$. Its matrix form is

$$X = \begin{pmatrix} 1 & 0 \\ 0 & 1 \end{pmatrix}. \tag{9}$$

R_y is a single-qubit rotation gate which has the form

$$R_y(\theta) = \begin{pmatrix} \cos\frac{\theta}{2} & -\sin\frac{\theta}{2} \\ \sin\frac{\theta}{2} & \cos\frac{\theta}{2} \end{pmatrix}, \tag{10}$$

where θ is the rotation angle. When acting on $|0\rangle$, the R_y-gate generates the following superposition state

$$R_y(\theta)\,|0\rangle = \cos\tfrac{\theta}{2} + \sin\tfrac{\theta}{2}\,|0\rangle\,.$$

C^nR_y is a multi-qubit controlled rotation gate, where n represents the number of control qubits. When the control qubits are all in $|1\rangle$, the R_y rotation operation is performed on the target qubit. The two-qubit controlled rotation gate CR_y with $n = 1$ is represented as

$$CR_y(\theta) = \begin{pmatrix} 1 & 0 & 0 & 0 \\ 0 & 1 & 0 & 0 \\ 0 & 0 & \cos\frac{\theta}{2} & -\sin\frac{\theta}{2} \\ 0 & 0 & \sin\frac{\theta}{2} & \cos\frac{\theta}{2} \end{pmatrix}. \tag{11}$$

The target qubit $|\varphi\rangle$ will undergo a $R_y(\theta)$ rotation if control qubits are in $|1\rangle$, that is,

$$C^nR_y(\theta)\,|1\rangle_c^{\otimes n}\,|\varphi\rangle_t = |1\rangle_c^{\otimes n}\,R_y(\theta)\,|\varphi\rangle_t\,,$$

where subscript c represents the control qubit and t stands for the target qubit.

A. Naïve-QBC

A QBC uses Bayes' rule to perform classification tasks within the framework of quantum computing. A single-qubit can be used to represent a node in a Bayesian network, and then a superposition quantum state can be used to represent the probability of different label values under various combinations of attributes in the Bayesian network, i.e., $P(y|X)$.

In a naïve Bayesian network, all attributes are independent of each other they depends only on the label. Let n attribute nodes be x_1, x_2, $\cdots$, x_n, and each attribute depends only on the label y. The quantum circuit of the naïve-QBC is composed of $n+1$ qubits, corresponding to the label y and n attribute nodes x_1 to x_n. The naïve-QBC is constructed as follows:

(a) All $n+1$ qubits are initialized to $|0\rangle$.

(b) For the label node y, the *class-prior probability* $P(y=0)$ can be obtained by statistically counting the training set. After that, one can encode the class-prior probabilities by $R_y(\cdot)$ operation. Unlike the encoding function arctan used in the Ref. [27], we use a more natural way of encoding. That is, let

$$\cos^2\tfrac{\theta}{2} := P(y=0). \tag{12}$$

One can obtain

$$\theta = 2\arccos\sqrt{P(y=0)}. \tag{13}$$

This achieves quantum encoding of the *class-prior probabilities*. To simplify the representation in the following content, let

$$f(P) := 2\arccos\sqrt{P}. \tag{14}$$

(c) For each attribute node x_i, one can get the *class-conditional probabilities* by statistically calculating $P(x_i = 0|y=1)$ and $P(x_i=0|y=0)$. Then, these probabilities are encoded by $CR_y(\cdot)$, where the controlled rotation angles are set as $\theta_{i+1} = f(P(x_i=0|y=1))$ and $\theta_{i+n+1} = f(P(x_i=0|y=0))$, respectively.

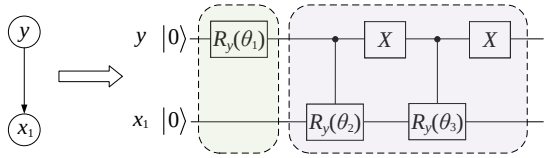

FIG. 2: The quantum circuit for $y \to x_1$, i.e., the naïve-QBC with only one attribute ($n = 1$).

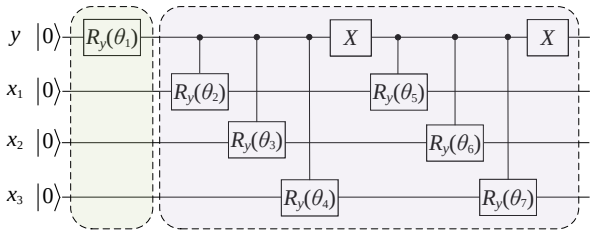

FIG. 3: The naïve-QBC with 3 attributes. Quantum circuits of QBCs.

Take the naïve Bayesian network in Fig. 1a as an example. Suppose these are one label node y and one attribute node x_1 ($n = 1$), and each node has only 2 values, either 0 or 1. By statistically counting the *class-prior probabilities* $P(y = 0)$ and the *class-conditional probabilities* $P(x_1 = 0|y = 1)$ and $P(x_1 = 0|y = 0)$, one can construct a quantum circuit as depicted in Fig. 2. In this case, the output of the circuit is

$$\sum_{i,j=\{0,1\}} \sqrt{P(y=i)}\sqrt{P(x_1=j|y=i)}\,|ij\rangle\,. \tag{15}$$

Note that the probabilities of different label values and attribute values are encoded in the amplitude of the output state, which is the same as Eq. (7). That is, the quantum circuit implements the naïve-QBC for features with only one attribute.

By continuously adding new attribute nodes to the quantum circuit and establishing controlled rotations between parent nodes and child nodes, one can construct QBCs based on different dependency relationships. Another example is a Bayesian network with multiple attributes. That is, the naïve QBC with $n = 3$ attributes is shown in Fig. 3.

In the prediction stage, for a given feature value X^*, one only needs to obtain the probabilities of the basis state $|y = i, X = X^*\rangle$ by measuring the output state of the naïve QBC. For a binary classification problem, one obtains the values of $P(y = 0, X = X^*)$ and $P(y = 1, X = X^*)$, and chooses the y value with a higher probability as the classification outcome of the QBC.

B. SPODE-QBC

For the SPODE Bayesian network, n attribute nodes are $x_1, x_2, \cdots, x_n$. Without loss of generality, assume that x_1 is the super-parent node, as shown in Fig. 1b. The quantum circuit of the SN-QBC based on the SPODE structure (SPODE-QBC) consists of $n + 1$ qubits, corresponding to y and x_1 to x_n. The construction of SPODE-QBC is as follows:

(a) All $n + 1$ qubits are initialized to $|0\rangle$.

(b) For the label node y, the *class-prior probability* $P(y = 0)$ is counted and encoded by $R_y(\cdot)$, where the rotation angle is set as $\theta_1 = f(P(y = 0))$.

(c) For the super-parent x_1, one needs to count the *class-conditional probabilities* $P(x_1 = 0|y = 0)$ and $P(x_1 = 0|y = 1)$ and encode these probabilities by using X and $CR_y(\cdot)$, with the controlled rotation angles being set as $\theta_2 = f(P(x_1 = 0|y = 1))$ and $\theta_3 = f(P(x_1 = 0|y = 0))$, respectively.

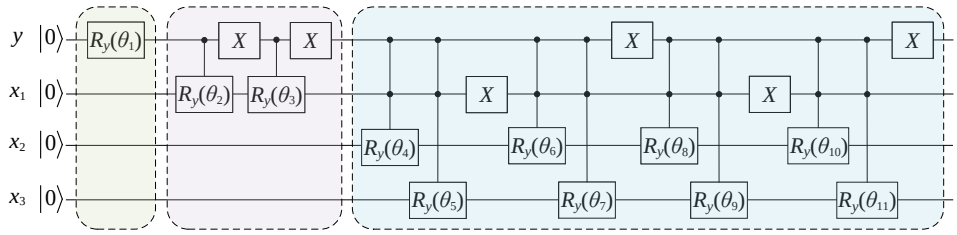

FIG. 4: The quantum circuit of the SPODE-QBC with 3 attributes and x_1 as the super-parent node.

(d) For the remaining attributes x_2 to x_n, since each node has two parent nodes, four $C^2R_y(\cdot)$ are used to encode the corresponding *class-conditional probabilities* $P(x_j = 0|y, x_1)$, where the controlled rotation angles are set as $f(P(x_j = 0|y, x_1))$ given the values of y and x_1. That is, when the control bits are $yx_1 = 00, 01, 10, 11$, the corresponding controlled rotation angles are set as $f(P(x_j = 0|y = 0, x_1 = 0))$, $f(P(x_j = 0|y = 0, x_1 = 1))$, $f(P(x_j = 0|y = 1, x_1 = 0))$, and $f(P(x_j = 0|y = 1, x_1 = 1))$, respectively.

For example, for a SPODE structured Bayesian network with 3 attributes shown in Fig. 1b, the quantum circuit of the SPODE-QBC is depicted in Fig. 4. Specifically, the class-conditional probabilities of x_2, x_3, and x_4 are encoded as $\theta_4 = f(P(x_2 = 0|yx_1 = 11))$, $\theta_5 = f(P(x_3 = 0|yx_1 = 11))$, $\theta_6 = f(P(x_2 = 0|yx_1 = 10))$, $\theta_7 = f(P(x_3 = 0|yx_1 = 10))$, $\theta_8 = f(P(x_2 = 0|yx_1 = 00))$, $\theta_9 = f(P(x_3 = 0|yx_1 = 00))$, $\theta_{10} = f(P(x_2 = 0|yx_1 = 01))$, $\theta_{11} = f(P(x_3 = 0|yx_1 = 01))$. The output of the SPODE circuit is

$$\sum_{i,j,k,l=\{0,1\}} \sqrt{P(y=i)P(x_1=j|y=i)P(x_2=k|y=i,x_1=j)P(x_3=l|y=i,x_1=j)}\,|ijkl\rangle\,. \tag{16}$$

C. TAN-QBC

For a SN-QBC based on the TAN structure, one needs to obtain the TAN structure Bayesian network firstly. The TAN structure Bayes classifier is generated based on the maximum-weighted spanning tree algorithm [32, 37], which includes the following steps [32]:

(1) Calculate the conditional mutual information between any two nodes x_i and x_j using the following equation

$$I(x_i, x_j|y) := \sum_{x_i,x_j,c\in Y} P(x_i, x_j|c) \log \frac{P(x_i, x_j|c)}{P(x_i|c)P(x_j|c)}. \tag{17}$$

(2) Build a complete graph among nodes and set $I(x_i, x_j|y)$ as the weight between x_i and x_j.

(3) Construct the maximum-weighted spanning tree of the complete graph and set the direction of each edge outward from the root.

(4) Add the label node y and directed edges from y to each node.

For a Bayesian network with a TAN structure, the quantum circuit of the TAN-QBC consists of $n + 1$ qubits, corresponding to y and x_1 to x_n. The construction of TAN-QBC is as follows:

(a) All qubits are initialized to $|0\rangle$.

(b) The *class-prior probability* $P(y = 0)$ is encoded by $R_y(f(P(y = 0)))$.

(c) Starting from the root node of the feature spanning tree, the *class-conditional probabilities* of each node are encoded layer by layer. For attribute x_j, it has at most two parent nodes, i.e., y and x_{parent_j}, where x_{parent_j} is the parent node of x_j on the upper layer (note that the root node of the feature spanning tree only has one parent y). The *class-conditional probabilities* $P(x_j|y, x_{\text{parent}_j})$ are encoded into the circuit as the rotation angles of four $C^2R_y(\cdot)$ gates.

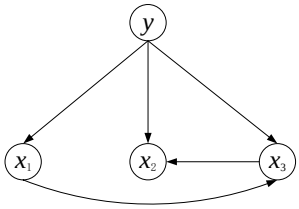

(a) The TAN structure Bayesian network.

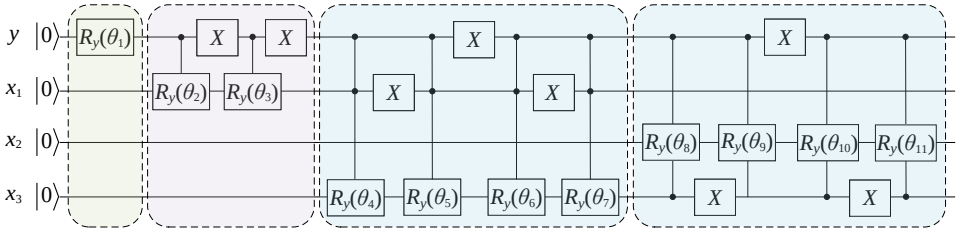

(b) The circuit of the TAN-QBC.

FIG. 5: The quantum circuit of the TAN-QBC based on the TAN structure Bayesian network.

A simple example of a Bayesian network with a TAN structure is given in Fig. 5a. While the circuit of the TAN-QBC based on the TAN structure is presented in Fig. 5b. The rotation angles of the label node y and the root node x_1 of the spanning tree are set as the naïive-QBCs shown in Sect. III A. The rotation angles of C^2R_y gates acting on x_3 are set as $\theta_4 = f(P(x_3 = 0|yx_1 = 11))$, $\theta_5 = f(P(x_3 = 0|yx_1 = 10))$, $\theta_6 = f(P(x_3 = 0|yx_1 = 00))$, and $\theta_7 = f(P(x_3 = 0|yx_1 = 01))$, respectively. While the rotation angles of C^2R_y gates acting on x_2 are set as $\theta_8 = f(P(x_2 = 0|yx_3 = 01))$, $\theta_9 = f(P(x_2 = 0|yx_3 = 00))$, $\theta_{10} = f(P(x_2 = 0|yx_3 = 10))$, and $\theta_{11} = f(P(x_2 = 0|yx_3 = 11))$, respectively. The output of the TAN structure SN-QBC is

$$\sum_{i,j,k,l=\{0,1\}} \sqrt{P(y=i)P(x_1=j|y=i)P(x_3=k|y=i,x_1=j)P(x_2=l|y=i,x_3=k)}\,|ijkl\rangle\,. \tag{18}$$

D. SN-QBC Based on the Symmetric Relationship of Image Attributes

Both the naïve Bayes classifier and the semi-naïve Bayes classifier only consider the dependencies between a small number of attribute nodes. Note that there are symmetric relationships among the sampled feature attributes in some images, such as the digits "6" and "9" shown in Fig. 6, where there exists symmetric relationships between attributes x_2 and x_5, and x_3 and x_4. These symmetric relationships of image attributes can be used to build Bayesian networks, which can then be used to establish corresponding SN-QBCs. The method for constructing a Bayesian network based on the symmetric relationships of image attributes is as follows.

(1) Establish a naïve Bayesian network as shown in Fig. 1a;

(2) Consider the symmetric relationship of attributes in the sample images and add a directed edge between each pair of attributes that are symmetrical to each other.

For example, for an image dataset of digits "6" and "9", a Bayesian network can be established as shown in Fig. 6.

For the Bayesian network with symmetric relationships between attributes, in the case of not considering the label node y, the network will consist of several independent trees. In this case, one can construct the corresponding symmetric-QBC by using the method for the TAN-QBC in Sect. III C. That is,

(a) Each node is initialized to $|0\rangle$.

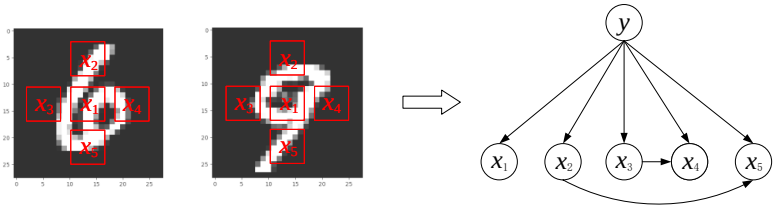

FIG. 6: The Bayesian network based on symmetric relationships of feature's attributes.

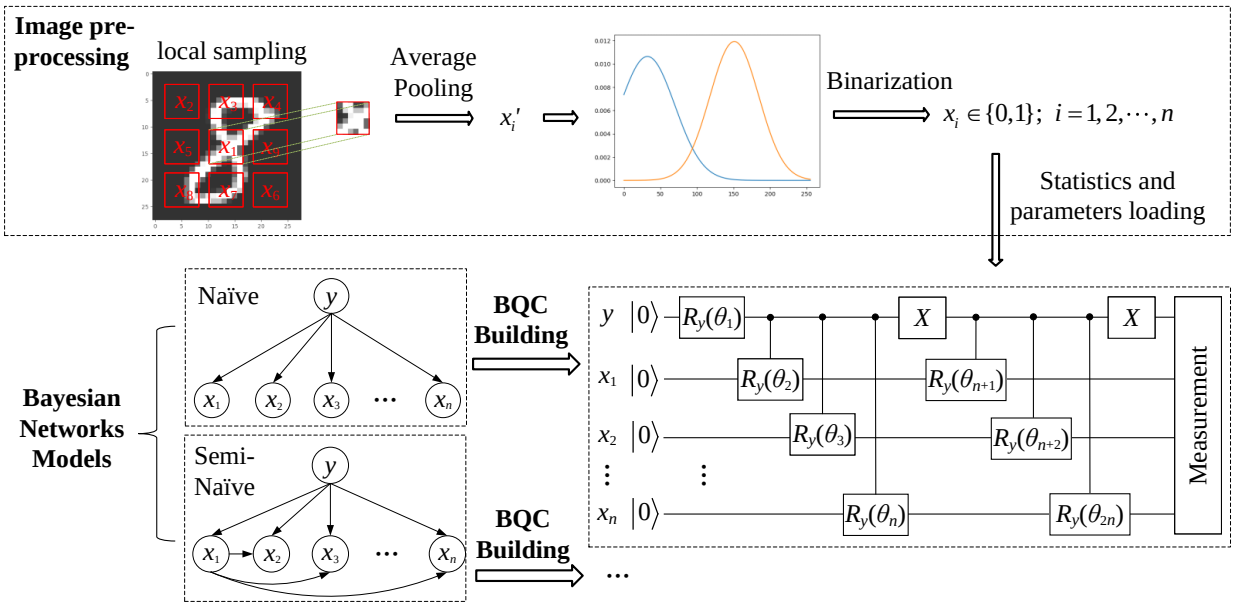

FIG. 7: The framework of image classifications based on QBCs.

(b) The *class-prior probability* $P(y=0)$ is encoded by $R_y(\cdot)$.

(c) Each independent tree is considered separately. For each tree, starting from the root node, the *class-conditional probabilities* of each node are encoded by $CR_y(\cdot)$ layer by layer, respectively.

IV. IMAGE CLASSIFICATION BASED ON QBCS

The key to the accuracy of a Bayesian classifier lies in feature selection and the structure of Bayesian networks. In this paper, we propose an image classification framework based on QBCs and local feature sampling, as illustrated in Fig. (7). Firstly, some local areas are selected in an image for feature sampling. Then, the sampled pixels are pooled and binarized to obtain local binary attributes of features. Finally, a QBC can be constructed based on a Bayesian network model with local attributes as nodes for image classification.

A. Local Feature Sampling

For image classifications using a naïve QBC, if each pixel of the image is taken as a node of a Bayesian network, the network will be very complex. For example, a 28*28 image requires 784 nodes to represent the network. Although n

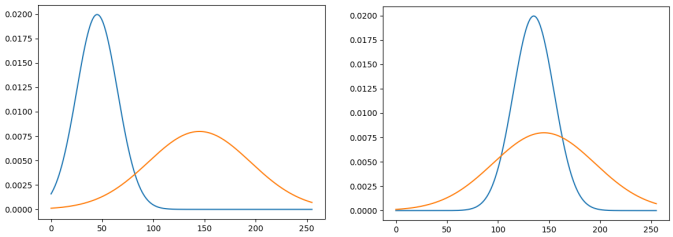

(a) One intersection. (b) Two intersections.

FIG. 8: Two Gaussian functions with intersections.

qubits can form a feature space with a dimension of 2^n, the resources required for the quantum Bayesian networks are still relatively large. In addition, considering the complex relationship of interdependence among feature's attributes, the complexity of Bayesian networks will continue to increase, which hinders the implementation of QBCs on current NISQ devices.

To reduce computational complexity and utilize features effectively for classification, we propose the local feature sampling method. This method aims to obtain a small number of local key attributes from an image. For image classification, background pixels shared by some images might not provide useful information for accurate classification by Bayes classifiers. The local feature sampling method can reduce the number of attribute nodes in Bayesian networks, decrease the scale and computational complexity of QBCs, and diminish the influence of quantum noise, which is beneficial for the experimental implementation of quantum circuits.

As for data preprocessing, the local feature sampling method is illustrated in Fig. 7, which is performed as follows.

(1) **Local sampling and average pooling**. Using a convolution operation on the sampling block and the convolution kernel, an image is locally sampled according to the specified block size (convolution kernel size). Next, the appropriate average pooling value x_i' of the attribute node x_i in the Bayesian network is obtained by applying average pooling [39].

(2) **Feature binarization**. In a classical Bayes classifier, assume that the probability density function $p(x_i|y) \sim N(\mu_{y,i}, \sigma_{y,i}^2)$, where $\mu_{y,i}$ and $\sigma_{y,i}^2$ are the mean and variance of the attribute x_i on the y-th class. One can obtain the *class-prior probability* by calculating the probability density function. However, it is challenging to replicate this process for a QBC. In this case, binarization is used to transform x_i into 0 or 1 such that it can be represented by a single-qubit.

Here, we use the maximum likelihood estimation (MLE) [40, 41] method adopted in classical Bayes classifiers for obtaining *class-conditional probabilities* of continuous variables. For the binary classification problem, this method runs as follows. Assume that $p(x_i|y_0) \sim N(\mu_{y_0,i}, \sigma_{y_0,i}^2)$ and $p(x_i|y_1) \sim N(\mu_{y_1,i}, \sigma_{y_1,i}^2)$. When two Gaussian functions have only one intersection, which is denoted as x_{ins}, as shown in Fig. (8a), the attribute value is set as follows

$$x_i = \begin{cases} 0, & \text{if } x_i' \le x_{\text{ins}} \text{ and } \mu_{y_0,i} \le \mu_{y_1,i}, \text{ or } x_i' > x_{\text{ins}} \text{ and } \mu_{y_0,i} > \mu_{y_1,i}; \\ 1, & \text{otherwise.} \end{cases} \tag{19}$$

where x_i' is the average pooling value generated by the the average pooling processing. If there are two intersections x_{ins1} and x_{ins2} with $x_{\text{ins1}} \le x_{\text{ins2}}$, as shown in Fig. (8b), in cases where $\mu_{y_0,i} \le \mu_{y_1,i}$, the attribute value is set as

$$x_i = \begin{cases} 0, & \text{if } x_i' \le x_{\text{ins1}}, \text{ or } x_{\text{ins1}} \le x_i' \le x_{\text{ins2}} \text{ and } |x_{\text{ins1}} - x_i'| \le |x_{\text{ins2}} - x_i'|; \\ 1, & \text{otherwise.} \end{cases} \tag{20}$$

Conversely, when $\mu_{y_0,i} > \mu_{y_1,i}$, the attribute value is set as

$$x_i = \begin{cases} 1, & \text{if } x_i' \le x_{\text{ins1}}, \text{ or } x_{\text{ins1}} \le x_i' \le x_{\text{ins2}} \text{ and } |x_{\text{ins1}} - x_i'| \le |x_{\text{ins2}} - x_i'|; \\ 0, & \text{otherwise.} \end{cases} \tag{21}$$

By utilizing the aforementioned method, it is possible to obtain a limited number of local attributes of features. These local attributes serve as nodes of Bayesian networks for the constructions of QBCs.

B. Image Classification Algorithm Based on QBCs

The image classification algorithm based on QBCs and local feature sampling is shown in Fig. (7). The algorithm consists of two stages, namely the image preprocessing stage, and the Bayesian networks and QBCs construction stage. In the image preprocessing stage, certain local areas are chosen for sampling. After that, the sampled attributes are pooled, and the Gaussian method is used for binarization. This process converts the sampled key attributes into either 0 or 1, allowing an attribute to be represented by a single-qubit in QBCs. In the second stage, a Bayesian network model is selected and the corresponding QBC is constructed with local key attributes as nodes. The algorithm runs as follows.

(a) A Bayesian network is selected.

(b) Local sampling and average pooling are performed on images from the training set, and the mean value μ_i and variance σ_i of the corresponding attributes are calculated. The Gaussian binarization method is executed to obtain the binarized attributes, as described in Sect. IV A.

(c) The QBC circuit is constructed based on the chosen Bayesian network model by using local binarized attributes as nodes. Also see Sect. III.

(d) The *class-prior probability* and *class-conditional probability* required for the Bayesian network are calculated statistically. These values are then loaded into the QBC circuit as controlled angles to complete the construction of the QBC.

(e) To predict the class of a new image, one needs to repeat the step (b) to obtain a new local key feature X' of the image, and then measures the probabilities of states $|0X'\rangle$ and $|1X'\rangle$ on the QBC circuit. The class with the highest probability will be the classification result of the image.

V. SIMULATIONS

In this paper, we simulate four QBCs on the MindQuantum [33] quantum simulation platform. And the performances of these QBCs are tested using the MNIST [34] and Fashion-MNIST [35] datasets. In the preprocessing stage, the sampling block size is set to 7*7, and the average pooling method is applied. All images are sampled according to the sampling positions shown in Fig. (9) to obtain 9 local key attributes ($n = 9$).

As is shown in Fig. (9), four Bayesian network models are used to construct four corresponding QBCs, i.e., the naïve QBC, the SN-QBC based on the SPODE structure (SPODE-QBC), the SN-QBC based on the TAN structure (TAN-QBC), and the SN-QBC based on the symmetric relationships of attributes (symmetric-QBC). For the TAN structures of the MNIST and Fashion-MNIST datasets, the spanning trees of the training data of the two datasets are calculated according to the maximum weighted spanning tree algorithm [32, 37] introduced in Sect. III C.

A. The Accuracy of Binary Classification

The MNIST and Fashion-MNIST datasets are used to verify the binary classification effects of four QBCs on every two image classes. Fig. 10 and Fig. 11 show the classification accuracies of the four QBCs in the MNIST and the Fashion-MNIST datasets, respectively.

It can be seen from Fig. 10 that the symmetric-QBC shows a better classification performance in most cases. While as is shown in Fig. 11, the SPODE-QBC shows better results in the Fashion-MNIST dataset in most cases, and the symmetric-QBC also exhibits better classification results on some data.

In addition, the simulation results show that QBCs still does not achieve ideal classification results for some data in these two datasets, which lies in the following reasons.

(1) The Bayesian network used in the simulation may not be suitable for all data. Different Bayesian networks should be considered for different data;

(2) The hyperparameters involved in the simulation, such as the sampling block size, the convolution kernel size, and the pooling method, etc., has a significant impact on the results, which should be selected carefully;

(3) Some attributes extracted from the local sampling and binarization procedure can not distinguish data from two classes very well. Other sampling and binarization methods could be considered.

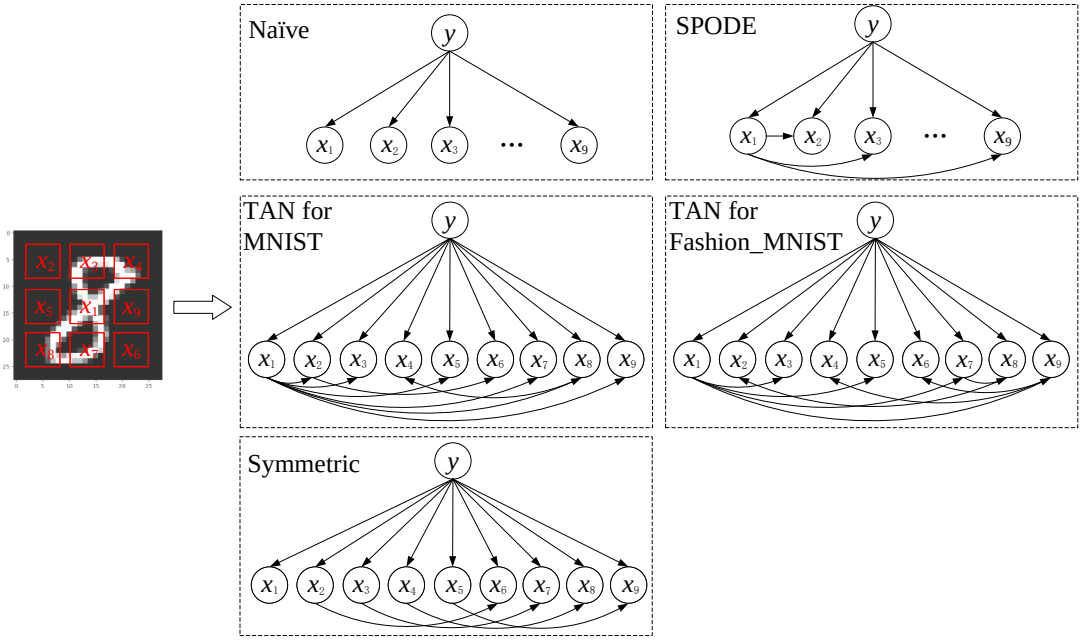

FIG. 9: The sampling points and four types of Bayesian networks used in the simulation, i.e., the naïve, the SPODE, the TAN, and the symmetric Bayesian networks.

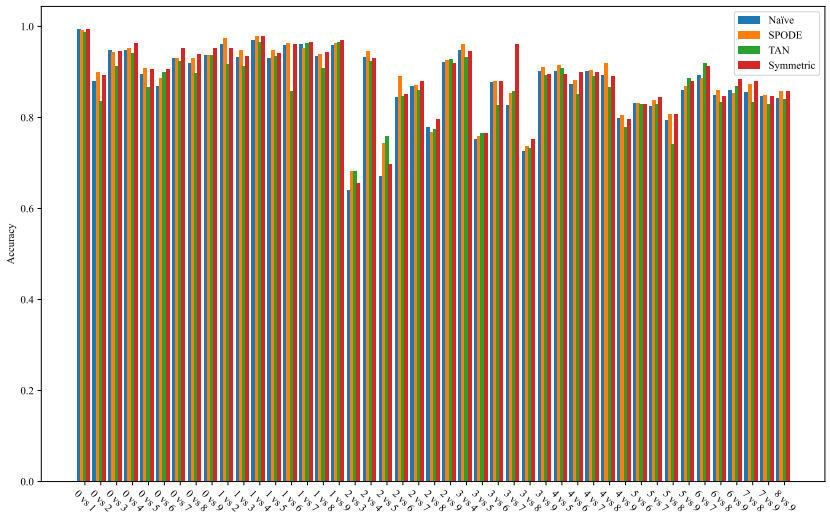

FIG. 10: The classification accuracies of every two classes in the MNIST dataset on the naïve QBC, the SPODE-QBC, the TAN-QBC, and the symmetric-QBC.

B. Overall Performance of QBCs

To evaluate the overall performance of each QBC, the average classification accuracy, variance, average precision, average recall, and average F_1 score [42, 43] are calculated. The average classification accuracy of a binary classifier

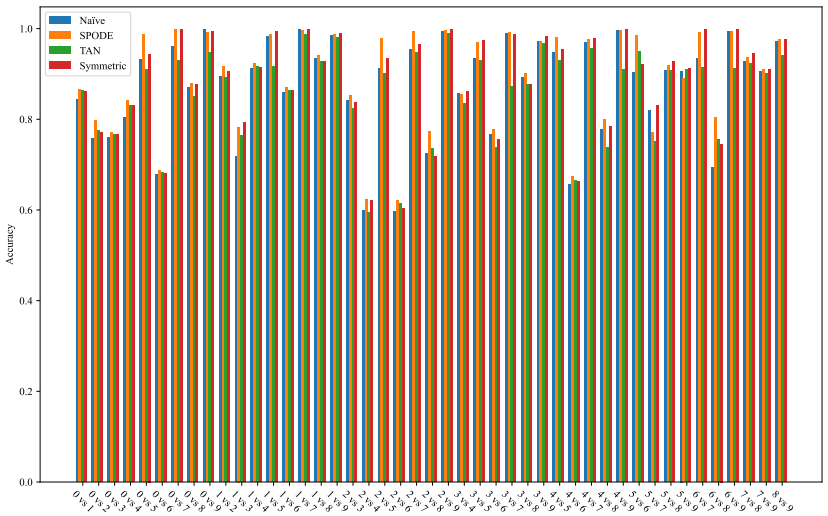

FIG. 11: The classification accuracies of every two classes in the Fashion-MNIST dataset on the naïve QBC, the SPODE-QBC, the TAN-QBC, and the symmetric-QBC.

for two classes in the MNIST and Fashion-MNIST datasets is defined as

$$\overline{acc} = \frac{1}{45}\sum_{i=0}^{8}\sum_{j=i+1}^{9} acc_{ij}, \tag{22}$$

where acc_{ij} represents the accuracy of binary classification of classes i and j. The variance is defined as

$$s^2 = \frac{1}{45}\sum_{i=0}^{8}\sum_{j=i+1}^{9} (\overline{acc} - acc_{ij})^2. \tag{23}$$

While the average precision, average recall, and average F_1 score are defined as

$$\overline{prec} = \frac{1}{45}\sum_{i=0}^{8}\sum_{j=i+1}^{9} \frac{TP_{ij}}{TP_{ij}+FP_{ij}}, \quad \overline{recall} = \frac{1}{45}\sum_{i=0}^{8}\sum_{j=i+1}^{9} \frac{TP_{ij}}{TP_{ij}+FN_{ij}}, \quad F_1 = \frac{2*\overline{prec}*\overline{recall}}{\overline{prec}+\overline{recall}}, \tag{24}$$

where TP means the number of true positive, FP means false positive, and FN means false negative. Table I shows the overall performance of the four QBCs mentioned above for all binary classification pairs in the MNIST and Fashion-MNIST datasets. As is shown in Table I, the SPODE-QBC and symmetric-QBC exhibit good classification accuracies in both the MNIST and Fashion-MNIST datasets, while the naïve-QBC and TAN-QBC also show relatively good classification effects. On the whole, the symmetric-QBC performs best in the MNIST dataset, while the SPODE-QBC performs best in the Fashion-MNIST dataset.

C. Comparison with Other Classifiers

Table II shows the comparison of classification performance of the classical Gaussian naïve Bayes classifier [44], the quantum convolutional neural network (QCNN) [14], and four QBCs for classes 0 and 1 in the MNIST and Fashion-MNIST datasets. The results show that QBCs performs better than the classical Bayes classifier and QCNN in the MNIST dataset, while the QCNN performs best in the Fashion-MNIST dataset. It is important to note that the classical Bayesian classifier and quantum neural network classifier use all 786 features, while the four QBCs in this paper use only 9 binary features. The simulation also shows that adjusting the sampling block size and the convolution kernels can improve the accuracy of QBCs, but this may not be effective for all classes of images. Specific analysis and adaptation are required for a specific task.

TABLE I: Overall performances of the four QBCs in two datasets.

Dataset	Classifier	$\overline{acc}$	s^2	$\overline{precision}$	$\overline{recall}$	F_1
MNIST	Naïve-QBC	0.8767	0.0777	0.8844	0.8689	0.8762
	SPODE-QBC	0.8873	**0.0707**	**0.8930**	0.8808	0.8864
	TAN-QBC	0.8055	0.0888	0.7390	**0.9775**	0.8388
	Symmetric-QBC	**0.8889**	0.0739	**0.8930**	0.8813	**0.8867**
Fashion-MNIST	Naïve-QBC	0.8712	0.1128	0.8726	0.8748	0.8728
	SPODE-QBC	**0.8916**	**0.1080**	**0.8863**	0.9107	**0.8962**
	TAN-QBC	0.8739	0.1115	0.8343	**0.9602**	0.8894
	Symmetric-QBC	0.8834	0.1112	0.8807	0.8942	0.8859

TABLE II: Comparison of classification accuracy of classes 0 and 1 in MNIST and Fashion-MNIST by different classifiers.

Classifier	MNIST 0 vs 1	Fashion-MNIST: 0 (t-shirt) vs 1 (trouser)
Classical naïve Bayes [44]	0.985	0.897
QCNN[14]	0.987	**0.941**
Naïve-QBC	**0.994**	0.844
SPODE-QBC	0.992	0.866
TAN-QBC	0.968	0.820
Symmetric-QBC	**0.994**	0.861

VI. DISCUSSIONS & CONCLUSIONS

In this paper, we study the constructions of QBCs using Bayesian networks. Based on four kinds of Bayesian networks, four QBCs are implemented, that is, the naïve-QBC, the SPODE-QBC with the attribute in an image center as the 'superparent', the TAN-QBC, and the symmetric-QBC. We apply these QBCs to image classification and propose the image classification algorithm. To reduce the computational complexity, a local feature sampling method is designed to extract a few key attributes from a huge number of image pixels. By retaining essential attributes, this method achieves high classification accuracies while reducing the feature size. Adjusting the sampling block size and utilizing different convolution kernels can further improve the accuracies of QBCs.

The classification effects of QBCs are verified on the MindQuantum platform for the MNIST and Fashion-MNIST datasets, respectively. The results show that QBCs perform well for image classification. We also compare QBCs with the classical Bayesian classifier and QCNN that use much larger size of features, which shows that QBCs using a fewer size of features still have advantages in some cases. Unlike QCNN classifiers [12, 14], QBCs do not require a time-consuming training process. They only require to calculate the corresponding parameters statistically and load them into quantum circuits, while the classification decision can be made by measuring quantum circuits, which is faster, lower in computational complexity, and less resource-consuming than QCNN. At present, there does not exist a general QBC model that performs well with all types of data. Building QBCs based on alternative varieties of Bayesian networks that work well with various datasets would be intriguing.

DATA AVAILABILITY STATEMENT

The data that support the findings of this study are available from the corresponding author upon reasonable request.

ACKNOWLEDGEMENTS

This project was supported by the National Natural Science Foundation of China (Grant No. 61601358).

[1] K. Mosegaard, M. Sambridge, Monte carlo analysis of inverse problems, Inverse Probl., 2002, 18(3), R29
[2] M. Modarres, K. Groth, *Reliability and risk analysis* (CRC Press, 2023)
[3] N. Daniels, Justice, health, and healthcare, Am. J. Bioeth., 2001, 1(2), 2
[4] P. Gary Jarrett, Logistics in the health care industry, Int. J. Phys. Distrib. Logist. Manag., 1998, 28(9/10), 741
[5] H. Wong, W. Lin, H. Laure, Multi-polarization reconfigurable antenna for wireless biomedical system, IEEE Trans. Biomed. Circuits Syst., 2017, 11(3), 652
[6] J. Kwisthout, Most probable explanations in bayesian networks: Complexity and tractability, Int. J. Approx. Reason., 2011, 52(9), 1452
[7] M. Chickering, D. Heckerman, C. Meek, Large-sample learning of bayesian networks is np-hard, J. Mach. Learn. Res., 2004, 5, 1287
[8] P.W. Shor, Polynomial-time algorithms for prime factorization and discrete logarithms on a quantum computer, SIAM J. Sci. Statist. Comput., 1997, 26(5), 1484
[9] L.K. Grover, Quantum mechanics helps in searching for a needle in a haystack, Phys. Rev. Lett., 1997, 79(2), 325
[10] P. Rebentrost, M. Mohseni, S. Lloyd, Quantum support vector machine for big data classification, Phys. Rev. Lett., 2014, 113(13), 130503
[11] Y. Dang, N. Jiang, H. Hu, Z. Ji, W. Zhang, Image classification based on quantum k-nearest-neighbor algorithm, Quantum Inf. Process., 2018, 17, 1
[12] I. Cong, S. Choi, M.D. Lukin, Quantum convolutional neural networks, Nat. Phys., 2019, 15(12), 1273
[13] I. Kerenidis, J. Landman, A. Prakash, Quantum algorithms for deep convolutional neural networks, arXiv preprint arXiv:1911.01117, 2019
[14] T. Hur, L. Kim, D.K. Park, Quantum convolutional neural network for classical data classification, Quantum Mach. Intell., 2022, 4(1), 3
[15] L.H. Gong, J.J. Pei, T.F. Zhang, N.R. Zhou, Quantum convolutional neural network based on variational quantum circuits, Opt. Commun., 2024, 550, 129993
[16] M. Schuld, F. Petruccione, Quantum ensembles of quantum classifiers, Sci. Rep., 2018, 8(1), 2772
[17] A. Macaluso, L. Clissa, L. Stefano, C. Sartori, Quantum ensemble for classification, arXiv preprint arXiv:2007.01028, 2020
[18] I.C. Araujo, A.J. Da Silva, Quantum ensemble of trained classifiers, in *2020 International Joint Conference on Neural Networks (IJCNN)* (IEEE, Glasgow, UK), 2020, pp. 1–8
[19] A. Macaluso, S. Lodi, C. Sartori, Quantum algorithm for ensemble learning, in *21st Italian Conf. Theoretical Computer Science (CEUR-WS.org, 2020)* 2020, pp. 149–154
[20] X.Y. Zhang, M.M. Wang, An efficient combination strategy for hybrid quantum ensemble classifier, Int. J. Quantum Inf., 2023, 21(06), 2350027
[21] W. Li, D.L. Deng, Recent advances for quantum classifiers, Sci. China Phys. Mech. Astron., 2021, 65(2), 220301
[22] S. Youssef, Quantum mechanics as an exotic probability theory, arXiv preprint quant-ph/9509004, 1995
[23] M. Ozols, M. Roetteler, J.R.M. Roland, Quantum rejection sampling, ACM Trans. Comput. Theory, 2013, 5(3), 1
[24] C. Moreira, A. Wichert, Quantum-like bayesian networks for modeling decision making, Front. Psychol., 2016, 7, 11
[25] S. Woerner, D.J. Egger, Quantum risk analysis, npj Quantum Inf., 2019, 1(5), 15
[26] G. Escrig, R. Campos, P.A.M. Casares, M.A. Martin-Delgado, Parameter estimation of gravitational waves with a quantum metropolis algorithm, Class. Quantum Grav., 2023, 40(4), 045001
[27] S.E. Borujeni, S. Nannapaneni, N.H. Nguyen, E.C. Behrman, J.E. Steck, Quantum circuit representation of bayesian networks, Expert Syst. Appl., 2021, 176, 114768
[28] W. Fathallah, N.B. Amor, P. Leray, An optimized quantum circuit representation of bayesian networks, in *European Conference on Symbolic and Quantitative Approaches with Uncertainty* (Springer, 2023), pp. 160–171
[29] I. Rish, Others, An empirical study of the naive bayes classifier, in *IJCAI 2001 workshop on empirical methods in artificial intelligence*, 2001, vol. 3, pp. 41–46
[30] K.M. Leung, Others, Naive bayesian classifier, Polytechnic University Department of Computer Science/Finance and Risk Engineering, 2007, 123
[31] I. Kononenko, Semi-naive bayesian classifier, in *Machine Learning—EWSL-91: European Working Session on Learning* (Springer, Porto, Portugal, 1991), pp. 206–219
[32] Z.H. Zhou, *Machine learning* (Springer Nature, 2021)
[33] M. Developer. Mindquantum, version 0.6.02021. URL `https://gitee.com/mindspore/mindquantum`
[34] Y. LeCun, L. Bottou, Y. Bengio, P. Haffner, Gradient-based learning applied to document recognition, Proc. IEEE, 1998, 86(11), 2278
[35] H. Xiao, K. Rasul, R. Vollgraf, Fashion-mnist: a novel image dataset for benchmarking machine learning algorithms, arXiv preprint arXiv:1708.07747, 2017

[36] J.O.R. Offmann-J O Rgensen, G. Pisier, The law of large numbers and the central limit theorem in banach spaces, Ann. Probab., 1976, pp. 587–599
[37] P.M. Camerini, The min-max spanning tree problem and some extensions, Inf. Process. Lett., 1978, 7(1), 10
[38] M.A. Nielsen, I.L. Chuang, *Quantum Computation and Quantum Information* (Cambridge University Press, Cambridge, UK, 2000)
[39] D. Yu, H. Wang, P. Chen, Z. Wei, Mixed pooling for convolutional neural networks, in *Rough Sets and Knowledge Technology: 9th International Conference, RSKT 2014*, pp. 364–375
[40] P. Dutilleul, The mle algorithm for the matrix normal distribution, J Stat. Comput. Simul., 1999, 64(2), 105
[41] M. Boull E, Modl: a bayes optimal discretization method for continuous attributes, Mach. Learn., 2006, 65, 131
[42] Y. Liu, Z. Yangming, A strategy on selecting performance metrics for classifier evaluation, Int. J. Mob. Comput., 2014, 6(4), 20
[43] O. Caelen, A bayesian interpretation of the confusion matrix, Ann. Math. Artif. Intell., 2017, 81(3–4), 429
[44] Gaussian naive bayes. URL `https://scikit-learn.org/stable/modules/generated/sklearn.naive_bayes.GaussianNB.html`